Proteolysis of Human Calcitonin in Excised Bovine Nasal Mucosa: Elucidation of the Metabolic Pathway by Liquid Secondary Ionization Mass Spectrometry (LSIMS) and Matrix Assisted Laser Desorption Ionization Mass Spectrometry (MALDI)

Steffen R. Lang,[1,7] Werner Staudenmann,[2] Peter James,[2] Hans-Jörg Manz,[3] Rudolf Kessler,[3] Bruno Galli,[4] Hans-Peter Moser,[5] Andreas Rummelt,[6] and Hans P. Merkle[1,8]

Received May 31, 1996; accepted August 23, 1996

Purpose. Two calcitonins, i.e. human calcitonin (hCT) and, for comparison, salmon calcitonin (sCT), were chosen as peptide models to investigate nasal mucosal metabolism.

Methods. The susceptibility of hCT and sCT to nasal mucosal enzymes was assessed by in-and-out reflection kinetics experiments in an *in vitro* model based on the use of freshly excised bovine nasal mucosa, with the mucosal surface of the mucosa facing the peptide solution. The kinetics of CT degradation in the bulk solution was monitored by HPLC. Peptide sequences of the main nasal metabolites of hCT were analyzed by using both liquid secondary ionization mass spectrometry (LSIMS), following HPLC fractionation of the metabolites, and matrix-assisted laser desorption ionization mass (MALDI) spectrometry. For sCT, the molecular weights of two major metabolites were determined by LC-MS with electrospray ionization.

Results. Both CTs were readily metabolized by nasal mucosal enzymes. In the concentration range studied metabolic rates were higher with hCT than with sCT. Presence of endopeptidase activities in the nasal mucosa was crucial, cleaving both calcitonins in the central domain of the molecules.

Conclusions. Typically, initial metabolic cleavage of hCT in nasal mucosa is due to both chymotryptic- and tryptic-like endopeptidases. The subsequent metabolic break-down follows the sequential pattern of aminopeptidase activity. Tryptic endopeptidase activity is characteristic of nasal sCT cleavage.

[1] Department of Pharmacy, Swiss Federal Institute of Technology Zurich (ETH), CH-8057 Zurich.
[2] Department of Biology, Laboratory of Biochemistry, Swiss Federal Institute of Technology Zurich (ETH), CH-8006 Zurich.
[3] Central Analytical Department, Ciba-Geigy AG, CH-4002 Basle.
[4] Research and Development, Ciba-Geigy AG, CH-4002 Basle.
[5] Central Analytical Department, Sandoz AG, CH-4002 Basle.
[6] Research and Development, Sandoz AG, CH-4002 Basle.
[7] Present address: Corporate Research Units, Ciba-Geigy AG, CH-4002 Basle.
[8] To whom correspondence should be addressed.

ABBREVIATIONS: MALDI-MS: matrix assisted laser desorption ionization mass spectrometry; LSIMS: liquid secondary ionization mass spectrometry; hCT: human calcitonin; sCT: salmon calcitonin; KBR: Krebs-Ringer buffer.

KEY WORDS: human calcitonin; salmon calcitonin; peptide metabolism; nasal metabolism; nasal mucosa; metabolic pathway; mass spectrometry; MALDI-MS; LSIMS; LC-MS.

INTRODUCTION

Information about the enzymatic cleavage positions and the metabolic pathways of nasally administered therapeutic peptides is so far typically available for small peptides only. For such peptides the number of potential metabolites caused by proteolytic activity is fairly low, and the metabolic pathway may thus be explored by using potential metabolites as reference substrates in comparative HPLC analyses of mucosal incubates. By this approach the metabolic pathways of Leuenkephalin (1), thymopentin (2) and thymocartin (3) in the nasal mucosa were elucidated. All three peptides were mainly cleaved by aminopeptidases leading to a step-wise degradation of the substrate peptide. Therefore, inhibition of aminopeptidases was suggested beneficial for the nasal delivery of such peptides. In contrast, the nasal metabolism of higher molecular weight peptides is neither well characterized nor understood.

For the analysis of peptide metabolites significant progress in peptide and protein sequencing during the last decade provided useful tools for peptide metabolism studies, particularly mass spectrometry (MS) techniques (4, 5). The usefulness of MS techniques was shown in several studies, e.g., by the use of electrospray-MS for the metabolism of hGH (4, 6) and the use of matrix assisted laser desorption ionization MS for analyses of hirudin metabolites (7).

The focus of the present study is on the investigation of the nasal metabolism of two polypeptides applicable for nasal therapy (8, 9): human calcitonin (hCT) and salmon calcitonin (sCT) as a reference. The study was designed (i) to gain more information about the proteases that are active in the nasal mucosa, and (ii) to compare the two CTs regarding their susceptibility to nasal metabolism.

For our studies, an *in vitro* model based on excised bovine nasal mucosa was used. This model membrane was shown before to be well suited for nasal metabolism studies (3, 10). By means of liquid secondary ionization mass spectrometry, LSIMS, and matrix assisted laser desorption ionization-MS, MALDI-MS, CT metabolites were analyzed to gain insight into the principal pathways of the nasal metabolism of the CTs.

MATERIALS AND METHODS

Chemicals

Human calcitonin (hCT, H-[Cys-Gly-Asn-Leu-Ser-Thr-Cys]-Met-Leu-Gly-Thr-Tyr-Thr-Gln-Asp-Phe-Asn-Lys-Phe-His-Thr-Phe-Pro-Gln-Thr-Ala-Ile-Gly-Val-Gly-Ala-Pro-NH_2, Ciba-Geigy AG, Basel, CH), molecular weight 3419 Da. Salmon calcitonin (sCT, H-[Cys-Ser-Asn-Leu-Ser-Thr-Cys]-Val-Leu-Gly-Lys-Leu-Ser-Gln-Glu-Leu-His-Lys-Leu-Gln-Thr-Tyr-Pro-Arg-Thr-Asn-Thr-Gly-Ser-Gly-Thr-Pro-NH_2, Sandoz AG, Basel, CH), molecular weight 3432 Da. Krebs Ringer buffer (KRB) was purchased from Sigma, Buchs, CH. The ion composition was (mM): $MgCl_2 \cdot 6H_2O$ 0.492; KCl 4.56; NaCl 119.8; Na_2HPO_4 0.70; NaH_2PO_4 1.5; $NaHCO_3$ 15. The *D*-glucose content was 10 mM. All KRB solutions were saturated with prehumidified carbogen (95% O_2/5% CO_2) prior to use.

0724-8741/96/1100-1679$09.50/0

Synthesis of FITC-18-hCT

Fluorescein isothiocyanate-18-hCT (FITC-18-hCT) was prepared as described by Arvinte et al. (11). Briefly, 900 μl of a solution of hCT in water (0.5 mg mL^{-1}) was given to 100 μl sodium carbonate buffer (0.5 M, 145 mM NaCl, pH 9.5) containing 0.4 mg FITC, shortly mixed on a vortex and incubated in the dark at room temperature for one hour. Excess FITC, not bound to hCT, was then separated from the reaction solution using a Sephadex (G25) column (Pharmacia, CH-Basle). The eluent was acetic acid (0.001%). The fractions containing the fluorophore-labelled peptide were identified by their fluorescence. Further isolation of FITC-18-hCT from the fluorescent fractions was done by preparative HPLC. The HPLC conditions were similar to those described below under HPLC system for fractionation of sCT metabolites. Unequivocal identification of FITC-18-hCT was done by LSIMS with chymotryptic digestion.

Excised Bovine Nasal Mucosa

Bovine nasal mucosa was obtained at the local slaughterhouse in Zurich (Schlachthaus AG, CH-Zurich) and prepared as described previously (3, 10). Particular care was taken to ensure near-perfect freshness and viability of the excised tissue during transport and separation of the mucosa from the underlying connective tissue and cartilage. Samples of 3–4 cm^2 size were obtained and inserted into the diffusion chambers, the mucosal side of the tissue routinely facing the bulk solution. For equilibration the mucosa was preincubated with KRB for 20 min.

Metabolism Kinetics

The metabolism of hCT and sCT was studied using a reflection kinetics model (3, 10). Briefly, only one half-cell of a side-by-side diffusion chamber set-up (3) was used. The other half cell was replaced by an impermeable acryl support block. This set up was adopted from Yu *et al.* (12). The nasal mucosa was inserted into the half cell, with the mucosal surface facing the peptide solution. By this set-up the flux of the peptide into the mucosa and the flux of the simultaneously formed metabolites were reflected at the impermeable support block. Steady-state loss of substrate was monitored in the bulk solution.

The KRB used for initial equilibration of the mucosa was replaced by 3 mL of a fresh solution of hCT or sCT in KRB, respectively. The temperature within the cells was maintained constant at 37°C via a thermal jacket, and the bulk solution was stirred (600 min^{-1}). Metabolism was studied at various peptide concentrations ranging from 1 to 60 nmol mL^{-1}. At given time intervals of up to 90 min samples were taken out of the bulk solution and analyzed by HPLC. The absence of significant release of proteolytic activity out of the mucosa into the bulk solution was verified by further incubation of bulk solution samples which were previously in contact to the mucosa.

The metabolic rates v_M [nmol cm^{-2} s^{-1}] of CTs were calculated from the linear parts of the concentration-time profiles $(dC/dt)_{ss}$ in the steady-state (ca. 0–60 min) according to Eq. 1.

$$v_M = -\left(\frac{dC}{dt}\right)_{SS} \frac{V}{A} \quad (1)$$

A [cm^2] = surface area of the model membrane, V [mL] = volume of the bulk solution.

To prepare samples for mass spectrometry the bulk solutions were incubated for a total of 60 min. Initial CT bulk concentrations were 12 nmol mL^{-1}. Samples were taken out of the bulk solution and were stored at −20°C until MS. Appropriate controls were made to verify the stability of the peptides under such storage conditions.

HPLC System for Reflection Kinetics Studies

The degradation kinetics of hCT and sCT were studied based on the HPLC method described by Buck and Maxl (13): The mobile phases consisted of a mixture of water:1M tetramethyl ammonium hydroxide: acetonitrile, 88:2:10 (*V/V/V*) for *A*, and 392:8:600 (*V/V/V*) for *B*. The pH of the mobile phases was adjusted to 2.5 with phosphoric acid. For analyses a linear gradient from 30% to 60% *B* in 25 min and a Lichrospher RP-18 (5 μm) column (Merck AG, CH-Basle) of 12.5 cm length were used. The HPLC system consisted of an autosampler AS2000, a gradient pump L-6200A, a UV detector L-4250 (λ = 214 nm) and an chromato-integrator D2500 (all Merck, CH-Basle).

HPLC System for Fractionation of hCT Metabolites

Prior to LSIMS analyses of hCT metabolites, fractionation of the samples of the incubation solution was performed on an Applied Biosystems Model 140B solvent delivery system (Applied Biosystems, CH-Basle). Approx. 360 μL of the incubation solution was injected onto a microbore OD-300 Aquapore column (1 mm × 100 mm). The mobile phases consisted of 0.1% (*V/V*) trifluoroacetic acid (TFA) for *A*, and 80% (*V/V*) acetonitrile in 0.08% (*V/V*) TFA for *B*. The peptides were eluted with a linear gradient (60 min) of 0–80% *B*. The flow rate was 50 μL min^{-1}. Column effluent was monitored at 214 nm. Fractions were collected over 60–90 s intervals. The fractions were speed-vac lyophilized and subsequently used for LSIMS.

HPLC System for Fractionation of sCT Metabolites

The HPLC system used was identical to that described under HPLC system for reflection kinetics studies. The fractionation of the incubation solution was performed by gradient elution. The mobile phases consisted of 0.1% (*V/V*) TFA and acetonitrile, 9:1 (*V/V*) for *A*, and 4:6 (*V/V*) for *B*. A flow rate of 0.5 mL min^{-1} of 40% *B* during 4 min followed by a linear gradient from 40% to 70% *B* in 20 min and a Lichrospher RP-18 (5 μm) column (Merck, CH-Basle) of 12.5 cm length were used. The injection volume was 400 μl.

Liquid Secondary Ionization Mass Spectrometry (LSIMS) of hCT Metabolites

Fast atom bombardment (FAB) mass spectra of hCT metabolites were recorded on a TSQ-700 triple quadrupole instrument (Finnigan MAT, San Jose, CA) equipped with a 15 kV cesium ion gun (Antek, Palo Alto, CA). Samples were prepared for MS analysis by dissolving the lyophilized HPLC

fractions in 0.1% TFA. Aliquots (0.5–1 μL, approx. 10–50 pmol) were introduced into the ion source on the gold plated tip (2 mm diameter) of a stainless steel probe. The tip was previously coated with a thin film of thioglycerol. Gas phase peptide ions $(M + H)^+$ were formed by bombardment of the sample matrix with 6–8 kV Cs^+ ions. The *m/z* range from 450 to 3000 was scanned in 4 s. Argon was used as the collision gas at a pressure of approximately 0.2 Pa in quadrupole 2. Peptide ions were fragmented at a collision energy of 10–25 V. The methodology employed for peptide sequence analysis by collision-activated dissociation (CAD) was similar to that described by Hunt *et al.* (4).

Electrospray (ESI) mass spectra were obtained on a Finnigan TSQ-700 instrument equipped with an Analytica ESI ion source (Brandford, CT-USA). Lyophilized HPLC fractions were redissolved in 0.1% TFA and introduced into the ion source with an infusion pump (Harvard Apparatus, South Natic, MS-USA). The sample flow rate was 2 μL min^{-1} together with a coaxial sheath liquid of 2-methoxyethanol at the same rate. Scans were acquired in profile mode in the *m/z* range of 400 to 2000 over the period of 4 s. Spectra were averaged for 1 min.

Methylation

In parallel to direct LSIMS of hCT metabolites LSIMS analyses of methylated hCT metabolites were also performed. Methylation was carried out with aliquots of the lyophilized HPLC fractions. Dried aliquots of HPLC fractions were reacted at room temperature for 90 min with 20 μL of a freshly prepared reagent solution of 2M HCl in methanol. The solvent was removed by speed-vac lyophilisation. For LSIMS the dry product was redissolved in 0.1% TFA.

Matrix Assisted Laser Desorption Ionization Mass Spectrometry (MALDI-MS) of hCT Metabolites

All measurements were done on a prototype (LDI 1700) instrument from Linear Scientific Inc. (Reno, USA). The ionizing and desorbing system consisted of a pulsed N_2-laser (λ = 337 nm, 250 μJ, 3 ns) with appropriate UV-optics. The separation stage consisted of a linear 1.7 m flight tube. For details see Börnsen et al. (14). For analyses typically 2 μL of the hCT incubation solution was mixed with 1 μL of an aqueous 0.1 mol L^{-1} acetonitrile solution of the matrix forming agent, sinapinic acid (3, 5-dimethoxy-4-hydroxy-trans-cinnamic acid). The measurements were made in the positive ion mode. Calibration was done by using human calcitonin (M = 3419) and hypertensin (M = 1032).

Liquid Chromatography-Mass Spectrometry (LC-MS)

LC-MS of sCT was done on a HP 1090 chromatograph (Hewlett Packard, Waldbronn, Germany) using a Spheri-5 RP18 column, 100 × 1 mm (Brownlee, CH-Basle). The HPLC method was already described above (HPLC system for fractionation of sCT metabolites). The flow rate was 50 μL min^{-1}. The injection volume was 100 μL. ESI mass spectra of sCT metabolites were recorded on a API III mass spectrometer (PE-Sciex, Thornhill, Ontario, Canada). The nebulizer pressure was 60 psi, and the interface temperature was 50°C. Detection was in the positive ion mode.

RESULTS

Reflection Kinetics Studies of hCT and sCT

hCT and sCT were readily metabolized in excised bovine nasal mucosa as indicated by additional peaks of metabolites on the HPLC chromatograms of CT solutions incubated *in vitro*. Controls showed that these additional peaks were neither present in KRB solutions incubated in the *in vitro* model, nor in CT solutions treated under similar conditions but without having contact with nasal mucosa (HPLC data not shown). The metabolic degradation of both CTs was studied at various concentrations from 1 to 60 nmol mL^{-1}. The metabolic rates (v_M) of both peptides were calculated from the linear parts of the concentration-time profiles for each concentration studied according to Eq. 1 and are demonstrated in Fig. 1. For hCT, the graph follows a saturation profile, i.e. non-linear kinetics were observed. The metabolic rates increased as a function of concentration and approach a plateau at higher concentrations.

For sCT, instead of a clear saturation profile as with hCT, we observed a more steady increase of the metabolic rates with increasing concentrations (Fig. 1). When comparing the two CTs, the metabolic rates of sCT were lower than those of hCT. This was must evident at the lower concentrations studied, e.g., at the initial CT concentration of 12 nmol mL^{-1} the ratio v_M (hCT) : v_M (sCT) was approx. 10:1, whereas at the highest concentration studied (60 nmol mL^{-1}) the ratio was much smaller (2:1).

Reflection Kinetics Studies of FITC-18-hCT

Corresponding studies on the metabolic degradation kinetics were performed with FITC-18-hCT. At the concentration studied (3 nmol mL^{-1}) the metabolic rate determined for FITC-18-hCT (v_M = 7.4 ± 0.63 · 10^{-4} nmol s^{-1} cm^{-2}, means ± SD, n = 4) was in the same range as for the native hCT (v_M = 6.9 · ± 0.23 · 10^{-4} nmol s^{-1}□$^{-2}$ means ± SD, n = 4).

LSIMS of hCT Metabolites

Prior to LSIMS analyses the hCT incubation solution was fractionated by HPLC. Ten fractions were collected. Each fraction was analyzed using electrospray ionization (ESI) and/or fast

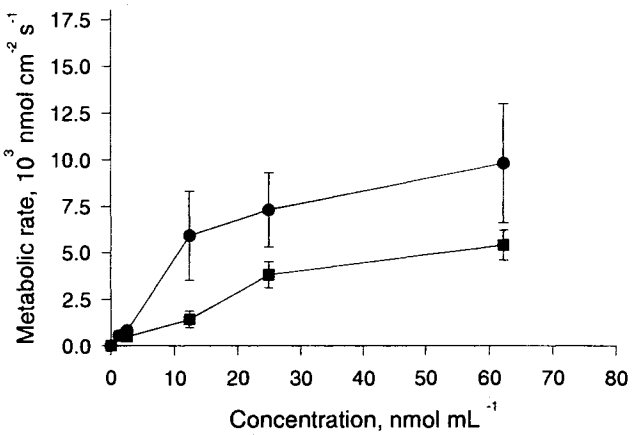

Fig. 1. Metabolic cleavage rates of sCT (■) and hCT (●) in excised bovine nasal mucosa (means ± SD, n = 4–6, error bars partly within symbols).

Table I. Nasal Metabolism of hCT. $(M+H)^+$ of Nasal hCT Metabolites Analyzed by LSIMS (FAB—nominal mass, ESI—average mass)

HPLC Fraction	FAB Native	FAB Methyl Ester	ESI Native	ESI Methyl Ester	hCT Fragment
1	512	512			27–32
2	583				26–32
3	684	684			25–32
4			826		1–8
5	1056	1056	1056	1056	22–32
	1157	1157			21–32
	1294	1294	1294	1294	20–32
6	1442		1442	1442	19–32
	1684		1684		17–32
7	939	953			1–9
	2337	2351			12–32
8	1994	2022			1–18
9			1751		1–16
10	2139		2140		1–19
			3417		1–32

atom bombardment (FAB). For comparative LSIMS analyses methylations of the HPLC fractions were done prior to MS analyses to identify N-terminal fragments of hCT. Table 1 shows the results of the FAB and ESI analyses for each collected HPLC fraction and the assigned hCT fragments resulting from the MS data. The assignment of the determined $(M + H)^+$ to the corresponding hCT fragments was verified by the interpretation of the CAD spectra of the native peptide and its methyl ester, respectively.

As an example a CAD spectrum for $(M + H)^+$ of mass 1294 used for the determination of the peptide sequence is shown in Table 2. The peptide sequence of the hCT fragment His^{20}-$ProNH_2^{32}$ can be read both from the *C*-terminus and the *N*-terminus (underlined data) with few exceptions. For His^{20}-$ProNH_2^{32}$ the molecular weight after incubation with the methylation solution was not different from that of the native metabolite before (Table I), because C-terminal methylation is blocked by the C-terminal amide of Pro^{32}. This was observed for all C-terminal fragments of hCT (Table I). As an exception, the fragment His^{12}-$ProNH_2^{32}$ showed the methyl ester mass shift caused by methylation of the free carboxyl group of Asp^{15}. For *N*-terminal fragments of hCT the methylation occurred at the free carboxyl group of the *C*-terminus, e.g., Cys^1-Leu^9 with a $(M + H)^+$ of 939 for the native peptide shifting to a mass of 953 after methylation.

MALDI-MS of hCT Metabolites

MALDI-MS analyses were performed directly from the hCT incubation solution. The resulting spectra contained signals of the $(M + H)^+$ ion of each peptide present in the incubation solution. The result of the MALDI-MS of a hCT incubation solution is shown in Table III. The incubation time was 60 min and the initial hCT concentration was 12 nmol mL^{-1}. Since in MALDI-MS spectra hCT metabolites may be overlaid with peaks of MALDI matrix ions in the *m/z* range from 0 to 700, interpretation of the spectra in this molecular weight range was neglected.

Metabolic Cleavage Pattern of hCT

In Fig. 2 the cleavage pattern of hCT in the nasal mucosa resulting from the LSIMS and MALDI-MS analyses is demonstrated. Metabolic cleavage of hCT (Fig. 2, top) in the nasal mucosa mainly occurs at three different regions in the molecule, i.e. between the amino acids no. 8–11, 16–21 and 24–26. In each region cleavage occurs at several peptide linkages. For the cleavage in the central segment of the peptide between Phe^{16}-Asn^{17}, Lys^{18}-Phe^{19}, Phe^{19}-His^{20} both the N- and the C-terminal counterparts were found simultaneously.

LC-MS Analyses of sCT Metabolites and Cleavage Pattern of sCT

sCT metabolism was analyzed by LC-MS only. In sCT solutions incubated with the nasal *in vitro* model only one additional peak of a potential metabolite was observed by HPLC (HPLC system for reflection kinetics studies, HPLC data not shown) in the first place. Optimization of the HPLC method and of the gradient applied (HPLC system for fractionation of sCT metabolites), however, resulted in a separation of the peak to form two separate peaks (HPLC data not shown). The molecular weight of the two potential metabolites were determined by LC-MS. The raw data showed the double and triple charged molecular ions. The masses reconstructed from the raw data for the two metabolites were 1957 and 1830. The two masses were indicative of the sCT fragments Cys^1-His^{17} and Cys^1-Lys^{18}, respectively. Fig. 2 (middle) shows the enzymatic cleavage position in sCT according to the analyzed fragments.

DISCUSSION

LSIMS and MALDI-MS of hCT Metabolites

The *in vitro* model used was previously developed by this group, and its feasibility demonstrated (3, 10). As shown in Tables I and III, the hCT metabolic cleavage pattern obtained with both techniques was similar. However, some metabolites found with LSIMS were not detected in MALDI-MS, i.e. the fragments Cys^1-Met^8, Cys^1-Leu^9, and His^{20}-$Pro^{32}NH_2$. The differences in the study protocol are likely to explain the contrasts. The fractionation and subsequent freeze drying of the incubation solutions prior to LSIMS analyses resulted in higher metabolite

Table II. Example of Collision-Activated Dissociation (CAD) for the Mass Peak m/z 1294. The Peptide Sequence of the hCT Fragment 20–32 [$(M+H)^+$ 1294] Is Verified by the Presence of the B and Y ions, that Are Underlined in the Panel

B	138	239	386	483	611	712	783	896	953	1052	1109	1180	1294	
	His	Thr	Phe	Pro	Gln	Thr	Ala	Ile	Gly	Val	Gly	Ala	Pro-NH_2	
	1294	1157	1056	909	812	684	583	512	399	342	243	186	115	Y

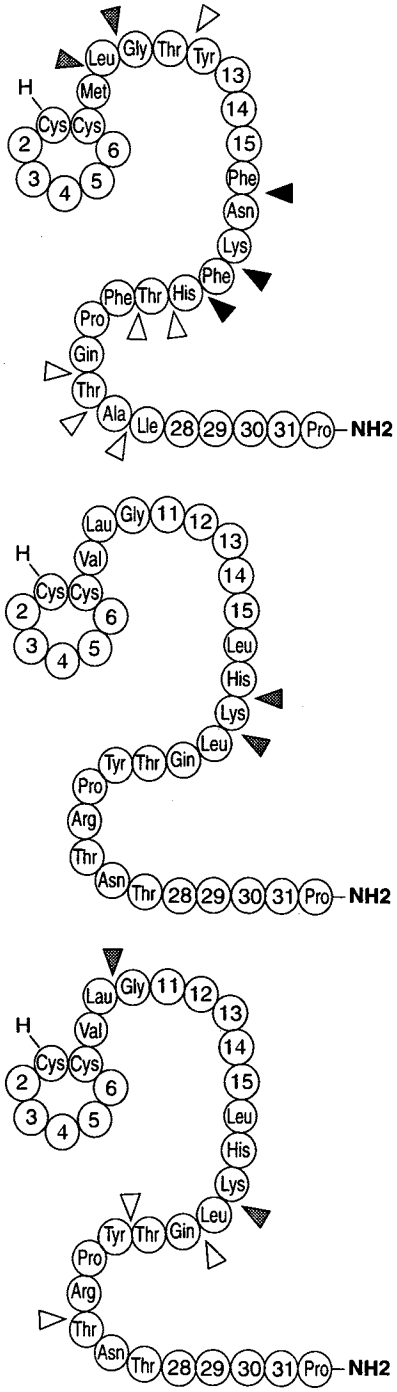

Fig. 2. *In vitro* nasal metabolism of hCT and sCT. *Top*: hCT in contact to excised bovine nasal mucosa, 60 min incubation. *Middle*: sCT in contact to excised bovine nasal mucosa, 60 min incubation. *Bottom*: sCT in homogenates of rabbit nasal mucosa from Dohi *et al.* (16), 4 h incubation. Arrowheads indicate metabolic cleavage positions (▶ = simultaneous N- and C-terminal fragments, ▻ = N-terminal fragment, ▷ = C-terminal fragment).

concentrations for LSIMS analyses, as compared to the native incubation solutions used for MALDI-MS analyses. Accuracy of MALDI generated data was lower than LSIMS data, particularly at the lower masses. As a consequence MALDI spectra require careful validation by more accurate MS techniques.

Table III. MALDI-MS Peak Spectrum of Nasal Metabolites, $(M + H)^+$, of Human Calcitonin (hCT). The Initial hCT Concentration of the Respective Metabolism Experiment Was 12 nmol mL^{-1}. The Incubation Time Was 60 min. For Comparison the Data of the Corresponding LSIMS Experiment (FAB and ESI) Is also Included (see Table I)

Peak No.	MALDI	LSIMS FAB	LSIMS ESI	Fragments
1	894.1			
		1294	1294	20–32
2	1433.6	1442	1442	19–32
3	1687.8	1684	1684	17–32
4	1753.9		1751	1–16
5	1994.2	1984		1–18
6	2141.9	2139	2140	1–19
7	2338.9	2337		12–32
8	3417.8		3417	1–32

The MALDI-MS peak of 894.1 could not be assigned to a hCT fragment. As this molecular weight was not detectable with LSIMS it is, therefore, supposed to be MALDI-MS generated, e.g., via the formation of adducts to the peak 826, that was analyzed by LSIMS (Table I) but not by MALDI (Table III).

For MALDI-MS analyses the native incubation solution was used directly, i.e. without further processing. Therefore, lengthy protocols as with LSIMS were avoided, e.g., the desalting of the samples and subsequent HPLC fractionation of metabolites. The time of analysis using MALDI-MS was cut down to a few minutes only. This may be the major advantage of MALDI-MS for routine use in metabolism kinetics studies, when properly validated e.g., by LSIMS.

Reflection Kinetics Studies of hCT and sCT

The results of the studies showed rate differences between both CTs (Fig. 1): sCT exhibited better stability when confronted with nasal enzymes than hCT. For hCT, the metabolic degradation followed a saturation profile, whereas for sCT the degree of saturation was minor. Based on this data no solid conclusions regarding differences of the cleavage mechanisms can be drawn. Such differences were, however, suggested from the analyses of the CT metabolites, where major differences were observed in the cleavage pattern and in the number of metabolites occurring with hCT and sCT (Fig. 2, top and middle).

Metabolic Cleavage of hCT

The cleavage positions suggested in hCT are characteristic for different types of enzymes (Fig. 2, top): Cleavage of hCT at the linkages Leu^9-Gly^{10}, Phe^{16}-Asn^{17} and Phe^{19}-His^{20} are indicative of chymotryptic enzyme activity. Tryptic enzyme activity corresponded to the cleavage at Lys^{18}-Phe^{19}. N-terminal cleavage of single amino acids seemed to occur with the fragment His^{20}-$ProNH_2^{32}$ resulting in stepwise cuts at Thr^{21}-$ProNH_2^{32}$ and then at Phe^{22}-$ProNH_2^{32}$, respectively. In analogy, Ala^{26}-$ProNH_2^{32}$ and Ile^{27}-$ProNH_2^{32}$ may by formed out of Thr^{25}-$ProNH_2^{32}$. This pattern is specific for aminopeptidases.

For the chymotrypsin- and trypsin-type cleavage of hCT at Phe^{16}-Asn^{17}, Lys^{18}-Phe^{19} and Phe^{19}-His^{20} both the *C*-terminal and *N*-terminal counterparts of the native peptide were identified at the

same time. Therefore, the cleavages at these linkages appear to represent the initial steps in the metabolic pathway of nasal hCT. On the other hand, metabolic rates remained essentially constant after introducing the bulky FITC side group at Lys^{18}.

For the cleavage at His^{20}-Thr^{21} and Thr^{21}-Phe^{22} only the C-terminal fragments, i.e. Thr^{21}-$ProNH_2^{32}$ and Phe^{22}-$ProNH_2^{32}$, were found, whereas the N-terminal counterparts were neither detected by LSIMS, nor by MALDI-MS. Therefore, Thr^{21}-$ProNH_2^{32}$ and Phe^{22}-$ProNH_2^{32}$ are not likely to be formed by primary cleavage of hCT, but by stepwise N-terminal aminopeptidase cleavage of His^{20}-$ProNH_2^{32}$. In analogy, the C-terminal fragments Ala^{26}-$ProNH_2^{32}$ and Ile^{27}-$ProNH_2^{32}$, that were observed in rather low concentrations in the incubation solution, as estimated from the relative peak areas on HPLC (fraction 1, 2, 3, Table I), may be formed by aminopeptidase cleavage of Thr^{25}-$ProNH_2^{32}$.

As a rather weak MS signal in fraction 7 the hCT fragment Tyr^{12}-$ProNH_2^{32}$, i.e. $(M + H)^+$ 2337, indicates that Thr^{11}-Tyr^{12} is no major cleavage site of hCT. The two N-terminal fragments Cys^1-Leu^9 and Cys^1-Met^8 may be formed secondary to the fragments Cys^1-Phe^{16}, Cys^1-Lys^{18} or Cys^1-His^{19}, or originate from the N-terminal counterpart Cys^1-Tyr^{11} of the C-terminal Tyr^{12}-$ProNH_2^{32}$. The N-terminal fragment Cys^1-Tyr^{11} itself was not detected in our studies, neither by LSIMS nor by MALDI-MS, but it is a likely intermediate in the metabolic pathway of hCT.

Metabolic Cleavage of sCT

The cleavage pattern of sCT showed much fewer cleavage positions as compared to hCT (Fig. 2, middle). The cleavage at Lys^{18}-Leu^{19} is indicative of tryptic endopeptidase activity. The fragment Cys^1-His^{17}, which was present at a higher concentration than Cys^1-Lys^{18}—as concluded from the relative HPLC peak areas (not shown)—may be either formed out of Cys^1-Lys^{18} by carboxypeptidase activity or directly out of the native sCT by nonspecific endopeptidase activity. Other metabolites, e.g., the C-terminal counterparts of the two metabolites mentioned were not detectable by HPLC, suggesting further degradation of such fragments by the nasal mucosal enzymes, e.g., by aminopeptidases.

Comparison of hCT and sCT Cleavage Patterns

Comparing the peptide sequences of hCT and sCT, there is a sequence homology of 16 amino acids (see Chemicals). In the central segment of hCT cleavage sites for chymotryptic enzymes are prominent as given by Phe^{16}-Asn^{17} and Phe^{19}-His^{20}. These cleavage sites do not exist in sCT, whereas the tryptic cleavage of sCT at Lys^{18}-Leu^{19} corresponds to Lys^{18}-Phe^{19} in hCT. Other linkages in hCT and sCT that may represent specific cleavage sites for tryptic and chymotryptic enzymes are Leu^9-Gly^{10} and Leu^{12}-Ser^{13} in sCT for tryptic and Tyr^{12}-Thr^{13} in hCT for chymotryptic activity. However, it is noteworthy that at these linkages no cleavage was detected. This may be indicative of a specificity of nasal tryptic and chymotryptic endopeptidases. Another possible explanation for the enzymatic stability of these linkages may be the secondary structure of the CTs. In both CTs the Cys^1-Cys^7 loop leads to perfect stability of the N-terminus against aminopeptidase cleavage. The importance of tryptic endopeptidase activity involved in the enzymatic degradation of nasal sCT, was previously confirmed by studies of Morimoto *et al.* (15). In their studies specific aminopeptidase and trypsin inhibitors were evaluated in rats. The best results were obtained by inhibition of the tryptic activity with aprotinin: The nasal bioavailabilities of sCT increased about two-fold as compared to control formulations without the inhibitor. In contrast, the inhibition of both the aminopeptidase and trypsin activity by camostate mesilate did not enhance sCT absorption confirming that nasal sCT is no primary substrate for aminopeptidases. In corresponding studies with vasopressin, nasal absorption rates were shown to be enhanced by aminopeptidase inhibition, but not by trypsin inhibition (15).

Thus the analyses of nasal sCT metabolites in our studies are fully consistent with the observations of Morimoto *et al.* (15). Moreover, the results of our studies on the cleavage pattern of sCT were recently confirmed by studies of Dohi et al. (16). Instead of using nasal mucosa directly, their investigations of the nasal metabolism of sCT was determined in mucosal homogenates of rabbits. In accordance to the data presented here sCT was shown to be cleaved at the Lys^{18}-Leu^{19} bond confirming the presence of an endopeptidase with tryptic activity in the nasal mucosa (Fig. 2, bottom).

In contrast to the studies in fully organized nasal mucosa presented here, the homogenate approach of Dohi *et al.* (16) indicated additional enzymatic cleavage positions, i.e. at Leu^9-Gly^{10}, Thr^{20}-Tyr^{21} and Arg^{23}-Thr^{24} (Fig. 2, bottom). Such cleavage positions are mainly indicative for chymotryptic endopeptidase activity. Furthermore, when using specific inhibitors of trypsin and chymotrypsin, only the inhibition of chymotryptic activity by chymostatin resulted in higher stability of sCT in the homogenate. The findings were confirmed by the same authors *in vivo* in rabbits: Nasal formulations containing chymostatin resulted in significant higher sCT bioavailabilities as compared to sCT formulations without inhibitor. Therefore, as concluded by Dohi et al. (16), chymotryptic endopeptidase activity represents the prime metabolic challenge for sCT in the nasal mucosa of rabbits.

The differences between the results in our studies and the studies of Dohi *et al.* (16), i.e. the differences in the cleavage pattern and in the number of cleavage positions observed in sCT (Fig. 2, middle versus bottom), may be explained by the experimental approach applied: In the homogenate approach of Dohi *et al.* (16) more enzymes that are present in the nasal mucosa may be active neglecting factors like the distribution of sCT and the metabolizing enzymes in the nasal mucosa. On the other hand the exclusively tryptic activity found in our mucosal studies may be explained by the location or the limited accessibility of other enzymatic activity in a fully organized cell matrix.

Another potential explanation for the higher number of metabolites observed in the studies with nasal homogenates in rabbits (16) may be the prolonged incubation time of 4h as compared to 60–90 min in our studies with excised nasal mucosa. The time period of 4h is unrealistic, because the half-life in the nasal cavity *in vivo* is only about 15–20 min due to fast muco-ciliary clearance. Finally, species differences cannot be excluded (bovine versus rabbit mucosae).

ACKNOWLEDGMENTS

The Ph.D. work of S. R. L. was generously supported by the Stipendienfonds der Basler Chemischen Industrie, Basel,

Switzerland. We also acknowledge the support of this work by both Ciba-Geigy AG, Basel and Sandoz AG, Basel.

REFERENCES

1. A. Hussain, J. Faraj, Y. Aramaki, and J. E. Truelove. *Biochem. Biophys. Res. Comm.* **133**:923–928 (1985).
2. M. A. Hussain, C. A. Koval, A. B. Shenvi, and B. J. Aungst. *Life Sci.* **47**:227–231 (1990).
3. S. Lang, R. Oschmann, B. Traving, P. Langguth, and H. P. Merkle. (TP4), *J. Pharm. Pharmacol.*, accepted for publication 1996
4. D. F. Hunt, J. R. Yates, J. Shabanowitz, S. Winston, and C. R. Hauer. *Proc. Natl. Acad. Sci. USA* **83**:6233–6237 (1986).
5. M. Karas and F. Hillenkamp. *Anal. Chem.* **60**:2301–2303 (1988).
6. V. J. Wroblewsky, R. E. Kaiser, and B. W. Becker. *Pharm. Res.* **10**:1106–1113 (1993).
7. F. Waldemeier, P. Graf, and M. Schär. Treffen Pharma-Peptide und Proteine, Zürich. (1993).
8. A. E. Pontiroli, M. Alberetto, A. Calderara, E. Pajetta, and G. Pozza. *Eur. J. Clin. Pharmacol.* **37**:427–430 (1989).
9. H. Kurose; Y. Seino, M. Shima, H. Tanaka., M. Ishida, K. Yamaopka, and H. Yabuchi. *Calcif. Tissue Int.* **41**:249–251 (1987).
10. G. Ditzinger, J. Sandow, and H. P. Merkle. *Proceed. Intern. Symp. Contr. Rel. Bioact. Mater.* **17**:220–221 (1990).
11. T. Arvinte, A. Cudd, and A. F. Drake. *J. Biolog. Chem.* **268**:6415–6422 (1993).
12. C. D. Yu, J. L. Fox, N. F. H. Ho, and W. I. Higuchi. *J. Pharm. Sci.* **68**:1347–1357 (1979).
13. R. H. Buck and F. Maxl. *J. Pharm. Biomed. Anal.* 8, Nos. **8–12**:761–769 (1989).
14. K. O. Börnsen, M. Schär, and E. Gassmann. *Biol. Mass Spectrom.* **20**:471–478 (1991).
15. K. Morimoto, M. Miyazaki, H. Yamaguchi, and M. Kakemi. *Proceed. Intern. Symp. Control. Rel. Bioact. Mater.* **19**:318–319 (1992).
16. M. Dohi, Y. Nishibe, Y. Makino, and Y. Suzuki. *Proceed. Intern. Symp. Control. Rel. Soc.* **P**:9, Kyoto, Japan (1993).